The Journal of Immunology

Hydroxylase Inhibition Selectively Induces Cell Death in Monocytes

Bianca Crifo, Bettina Schaible, Eric Brown, Doug N. Halligan, Carsten C. Scholz, Susan F. Fitzpatrick, Anna Kirwan, Helen M. Roche, Mattia Criscuoli, Antonella Naldini, Hugh Giffney, Daniel Crean, Alfonso Blanco, Miguel A. Cavadas, Eoin P. Cummins, Zsolt Fabian and Cormac T. Taylor

J Immunol 2019; 202:1521-1530; Prepublished online 30 January 2019;
doi: 10.4049/jimmunol.1800912
http://www.jimmunol.org/content/202/5/1521

The Journal of Immunology is published twice each month by
The American Association of Immunologists, Inc.,
1451 Rockville Pike, Suite 650, Rockville, MD 20852

Print ISSN: 0022-1767 Online ISSN: 1550-6606.

Hydroxylase Inhibition Selectively Induces Cell Death in Monocytes

Bianca Crifo,[*,†] Bettina Schaible,[†] Eric Brown,[†] Doug N. Halligan,[†] Carsten C. Scholz,[‡] Susan F. Fitzpatrick,[†] Anna Kirwan,[§,¶] Helen M. Roche,[§] Mattia Criscuoli,[‖] Antonella Naldini,[‖] Hugh Giffney,[†,#] Daniel Crean,[†,#,] Alfonso Blanco,[†] Miguel A. Cavadas,[††] Eoin P. Cummins,[*,†] Zsolt Fabian,[‡‡] and Cormac T. Taylor[*,†]**

Hypoxia is a common and prominent feature of the microenvironment at sites of bacteria-associated inflammation in inflammatory bowel disease. The prolyl-hydroxylases (PHD1/2/3) and the asparaginyl-hydroxylase factor-inhibiting HIF are oxygen-sensing enzymes that regulate adaptive responses to hypoxia through controlling the activity of HIF and NF-κB–dependent transcriptional pathways. Previous studies have demonstrated that the pan-hydroxylase inhibitor dimethyloxalylglycine (DMOG) is effective in the alleviation of inflammation in preclinical models of inflammatory bowel disease, at least in part, through suppression of IL-1β–induced NF-κB activity. TLR-dependent signaling in immune cells, such as monocytes, which is important in bacteria-driven inflammation, shares a signaling pathway with IL-1β. In studies into the effect of pharmacologic hydroxylase inhibition on TLR-induced inflammation in monocytes, we found that DMOG selectively triggers cell death in cultured THP-1 cells and primary human monocytes at concentrations well tolerated in other cell types. DMOG-induced apoptosis was independent of increased caspase-3/7 activity but was accompanied by reduced expression of the inhibitor of apoptosis protein 1 (cIAP1). Based on these data, we hypothesize that pharmacologic inhibition of the HIF-hydroxylases selectively targets monocytes for cell death and that this may contribute to the anti-inflammatory activity of HIF-hydroxylase inhibitors. ***The Journal of Immunology*****, 2019, 202: 1521–1530.**

Most eukaryotic cells require a constant supply of molecular oxygen to maintain bioenergetic homeostasis. Over the course of evolution, eukaryotic cells have evolved the capacity to adapt to conditions in which oxygen demand exceeds supply (hypoxia) (1). A key regulator of this response is a transcription factor termed the hypoxia-inducible factor (HIF), of which three isoforms have been described (HIF-1/2/3) (1). HIF is a heterodimeric protein consisting of an α-subunit, which is stabilized in hypoxia and a β-subunit, which is constitutively expressed (2). A family of three dioxygenases termed prolyl-hydroxylase domain (PHD) 1/2/3 and an asparagine hydroxylase, termed factor-inhibiting HIF (FIH), confer oxygen sensitivity upon HIF-α subunits through oxygen-dependent hydroxylation (3, 4). To hydroxylate HIF, these enzymes require molecular oxygen and α-ketoglutarate (α-KG) as cosubstrates and Fe^{2+} and ascorbate as cofactors (5).

In the presence of available oxygen, PHDs hydroxylate HIF-α, thereby promoting its interaction with the von Hippel–Lindau (pVHL) E3 ubiquitin ligase, which mediates its ubiquitylation and proteasomal degradation (6). In addition, FIH-dependent asparagine hydroxylation suppresses HIF-α in an oxygen-dependent manner by inhibiting its interaction with the transcriptional coactivator CBP/p300 and thus preventing its transactivation (7). In hypoxia, the HIF-hydroxylases are inactivated, resulting in HIF-α stabilization, transactivation, and dimerization with HIF-β to form a transcriptionally active HIF dimer (8). This complex translocates to the nucleus, interacts with transcriptional coactivators, and mediates the transcription of genes involved in adaptation to hypoxia (8).

In addition to regulating HIF, hydroxylases can regulate other transcriptional pathways, including NF-κB, which plays a critical role in the regulation of the inflammatory response (9). A wide range of stimuli regulate NF-κB, including growth factors, microbial products, and cytokines such as IL-1β and TNF-α (10, 11). After the causative stimulus is removed, NF-κB signaling is resolved to facilitate a return to tissue homeostasis through mechanisms, including the upregulation of A20 (encoded by the gene TNFAIP3) (12, 13).

*School of Medicine and Medical Science, University College Dublin, Belfield, Dublin 4, Ireland; †School of Biomolecular and Biomedical Science, Conway Institute of Biomolecular and Biomedical Research, University College Dublin, Belfield, Dublin 4, Ireland; ‡Institute of Physiology, University of Zürich, CH-8057 Zurich, Switzerland; §Nutrigenomics Research Group, Conway Institute of Biomolecular and Biomedical Research, University College Dublin, Belfield, Dublin 4, Ireland; ¶Institute of Food and Health, University College Dublin, Belfield, Dublin 4, Ireland; ‖Department of Molecular and Developmental Medicine, University of Siena, Siena, Italy; #School of Veterinary Medicine, University College Dublin, Belfield, Dublin 4, Ireland; **Diabetes and Complications Research Centre, University College Dublin, Belfield, Dublin 4, Ireland; ††Instituto Gulbenkian de Ciencia, Oeiras 2780-156, Portugal; and ‡‡Department of Medical Chemistry, Molecular Biology and Pathobiochemistry, Semmelweis University, H-1094 Budapest, Hungary

ORCIDs: 0000-0002-1360-2559 (B.S.); 0000-0001-6579-8015 (C.C.S.); 0000-0003-4194-908X (M.C.); 0000-0002-9600-2486 (A.N.); 0000-0003-0439-0838 (A.B.); 0000-0003-3917-9880 (M.A.C.); 0000-0002-9346-8299 (E.P.C.); 0000-0002-4973-9872 (Z.F.).

Received for publication July 2, 2018. Accepted for publication December 19, 2018.

This work was supported by grants from Science Foundation Ireland (11/PI/1005) and the European Union (15/ERA-CSM/3267).

Address correspondence and reprint requests to Prof. Cormac T. Taylor, Conway Institute, University College Dublin, Belfield, Dublin 4, Ireland. E-mail address: cormac.taylor@ucd.ie

The online version of this article contains supplemental material.

Abbreviations used in this article: BMDM, bone marrow–derived macrophage; DMOG, dimethyloxalylglycine; EDHB, ethyl-3,4-dihydroxybenzoate; FIH, factor-inhibiting HIF; HEK, human embryonic kidney; HIF, hypoxia-inducible factor; IAP1, inhibitor of apoptosis 1; IKK, IκB kinase; JNJ1935, JNJ-42041935; α-KG, α-ketoglutarate; LDH, lactate dehydrogenase; MEF, mouse embryonic fibroblast; PHD, prolyl-hydroxylase domain; PI, propidium iodide; Q-VD, 5-(2,6-difluorophenoxy)-3-[[3-methyl-1-oxo-2-[(2-quinolinylcarbonyl) amino]butyl]amino]-4-oxo-pentanoic acid hydrate; YP, YoPro.

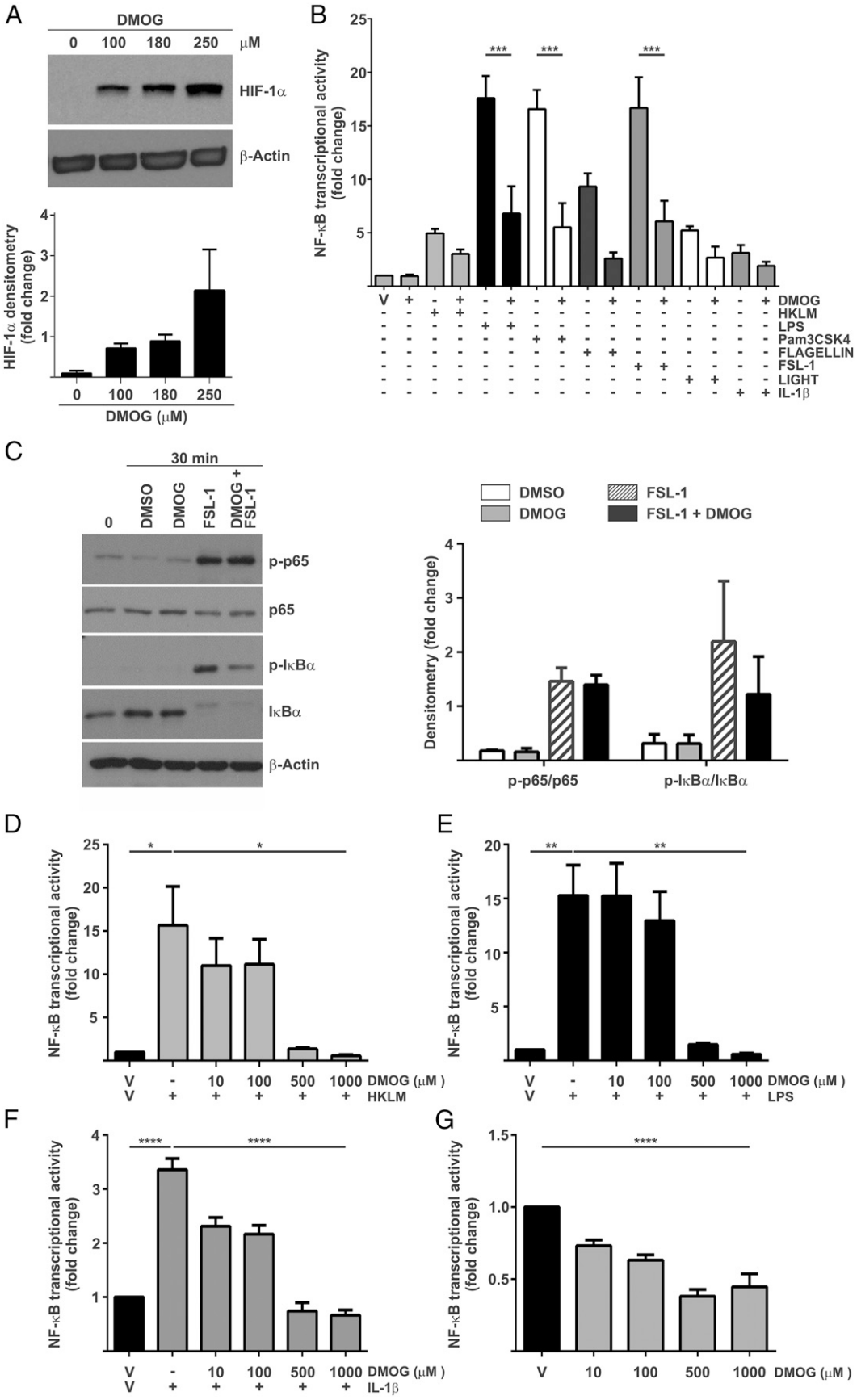

FIGURE 1. Hydroxylase inhibition attenuates TLR-mediated NF-κB activity. (**A**)THP-1$^{NF\text{-}\kappa B}$ cells were treated with 100–250 μM DMOG for 24 h, and HIF-1α or β-actin levels were determined by Western blot. Densitometry values are shown as mean + SEM for $n = 3$ independent experiments. (**B**) THP-1$^{NF\text{-}\kappa B}$ cells pretreated with 250 μM DMOG or with vehicle (V). After 1 h, cells were treated with 10^9 cells/ml HKLM, 1 μg/ml LPS, 1 μg/ml Pam3CSK4, or 1 μl/μg FLA-ST or 1 μl/μg FSL-1, 1 μg/ml LIGHT, or 10 ng/ml IL-1β for 24 h. Luciferase activity was measured by *(Figure legend continues)*

Both basal and cytokine-induced NF-κB activity are affected by pharmacologic hydroxylase inhibition in epithelial cells (14, 15). These observations led us to the hypothesis that HIF-hydroxylase inhibitors may effectively modulate the inflammatory response (16).

Pharmacologic hydroxylase inhibitors such as dimethyloxalylglycine (DMOG) and JNJ-42041935 (JNJ1935) are α-KG mimetics, which compete with endogenous α-KG for the binding to the catalytic sites of HIF-hydroxylases, thereby inhibiting them (17, 18). Other hydroxylase inhibitors, such as ethyl-3,4-dihydroxybenzoate (EDHB), regulate enzyme activity through the chelation of iron (17, 19). In murine models of colitis, pharmacologic hydroxylase inhibition reduces intestinal inflammation, at least in part, through reduced apoptosis of epithelial cells, resulting in enhanced barrier function (20). Despite their anti-inflammatory effects, the impact of pharmacologic hydroxylase inhibitors directly on inflammatory cells remains poorly understood.

In colitis, epithelial barrier dysfunction exposes monocytes in the lamina propria to bacteria from the intestinal microbiota, which are recognized through TLRs (21). To date, 10 members of the TLR superfamily have been described in humans. They recognize a broad range of microbial motifs and elicit a defensive immune response accordingly (22). Their extracellular leucine-rich-repeat is involved in the recognition of pathogen-associated molecular patterns or nucleic acids, whereas the intracellular Toll/IL-1 (TIR) domain activates downstream signaling pathways (10, 23, 24). The TIR domain is also present in the type 1 IL-1R, therefore, IL-1R1 and TLRs share multiple components and activate similar downstream signaling pathways through the common adaptor MyD88 (25, 26, 27). MyD88-mediated signal transduction culminates in activation of the MAPK and NF-κB pathways (28). Because of the therapeutic potential of hydroxylase inhibitors, the vital role of TLR activation during active colitis and the shared signaling pathway with the IL-1R pathway, in this study, we hypothesized that hydroxylase inhibition may regulate TLR-induced signaling and, consequently, inflammatory responses in human monocytes.

Materials and Methods

Cell culture

Human embryonic kidney (HEK) 293 cells, immortalized mouse embryonic fibroblast (MEF), T lymphocytes (Jurkat T cells), bone marrow–derived macrophages (BMDMs), and human monocytes (THP-1) were cultured using standard conditions.

Reagents

DMOG was obtained from Cayman Chemical (catalog no. 71210; Ann Arbor, MI). EDHB was obtained from Sigma-Aldrich (catalog no, E24859; St. Louis, MO). JNJ1935 was obtained from Johnson & Johnson (La Jolla, CA). The 5-(2,6-difluorophenoxy)-3-[[3-methyl-1-oxo-2-[(2-quinolinylcarbonyl) amino]butyl]amino]-4-oxo-pentanoic acid hydrate (Q-VD) was obtained from APExBIO (catalog no. A1901; Boston, MA). TLR ligands were purchased from InvivoGen (catalog no. tlr-kit1hw; San Diego, CA). For the investigation of the TNF pathway, human LIGHT (catalog no. SRP3106; Sigma-Aldrich) was used. For investigation of IL-1β signaling, IL-1β (catalog no. 201-LB; R&D Systems, Minneapolis, MN) was used.

Isolation of BMDMs

Male C57BL/6 mice were obtained from Envigo. All experiments were carried out with prior ethical approval from University College Dublin Animal Research Ethics Committee, and mice were maintained according to European Union and Irish Department of Health regulations. BMDMs were isolated from the tibias and fibulas of these mice and maintained as previously described (29).

Isolation of human monocytes

Peripheral venous blood was collected from healthy volunteers. Institutional approval was obtained from the ethics committee at St. Vincent's University Hospital and written informed consent was obtained from all volunteers. Thirty-two milliliters of heparinized blood was layered slowly onto Polymorphprep solution (catalog no. 1114544; Axis-Shield Diagnostics) (1:1) and centrifuged at 500 × *g* at 20°C for 35 min with the brake off. The mononuclear layer was removed and mixed with equal volumes of 0.45% NaCl by gentle inversion, followed by centrifugation at 300 × *g* at 20°C for 5 min with the brake on. Supernatant was discarded, and the pellet was resuspended in 3 ml of homemade isolation buffer containing 5× PBS, 2.5% BSA, and 10 mM EDTA and diluted in water to a final concentration of 1×. The PBMCs were counted and reconstituted in 100 μl aliquots of 1.5×10^7 cells/ml. Monocyte isolation was carried out using the MojoSort Human $CD14^+$ Monocyte Isolation Kit (catalog no. 480047; BioLegend). After isolation, PBMCs and isolated monocytes were collected and spun at 500 g for 4 min and resuspended in 200 μl aliquots of cell-staining buffer (catalog no. 420201; BioLegend) at a density of 2×10^6 cells/ml. $CD14^+$ FITC (catalog no. 301803; BioLegend) and $CD16^-$ PE Abs (catalog no. 302007; BioLegend) were added to the cells at a 1:66 dilution and incubated on ice in the dark for 30 min. Cells were spun at 500 g for 4 min, and the pellet was washed in the cell-staining buffer twice. Unstained, $CD14^+$ and PBMCs were analyzed by flow cytometry, using the BD Accuri C6 flow cytometer (BD Bioscience, Oxford, U.K.) and CFlow software (version 1.0.264.21).

THP-1$^{NF\text{-}\kappa B}$

THP-$1^{NF\text{-}\kappa B}$ were derived from THP-1 human monocyte cell line by stable integration of an NF-κB, Luc-inducible reporter construct. These cells were obtained from InvivoGen (San Diego, CA).

Luciferase assay

A total of 1×10^5 THP-$1^{NF\text{-}\kappa B}$ cells were seeded in 96-well plate in a final volume of 180 μl. Cells were incubated with the indicated hydroxylase inhibitor. After 1-h treatment, a range of concentrations of TLR agonists were diluted to a final volume of 20 μl and added to each well. Ten microliters of medium was collected from the supernatant, and secreted luciferase activity was measured using BioLux Gaussia Luciferase Assay Kit (catalog no. E3300L; New England Biolabs, Ipswich, MA), according to the manufacturer's instructions. The luciferase activity was normalized to protein content.

Western blot

Protein concentrations of cell lysates for Western blot analyses were quantified using the Bio-Rad DC Protein Assay. Equal quantities of proteins were resolved by SDS-PAGE and transferred to nitrocellulose membranes. Immunoblot analyses were performed using Abs against HIF-1α (610958, 1:500, mouse; BD Biosciences), β-actin (A5316, 1:10,000, mouse; Sigma-Aldrich), c–inhibitor of apoptosis 1 (IAP1) (D5G9) (7065S, 1:1000, rabbit; Cell Signaling), phospho-RIP (Ser166) (D1L3S) (65746S, 1:1000; Cell Signaling), RIP (D94C12) XP (3493S,1:1000, rabbit; Cell Signaling), phospho-P65 (3033, 1:1000 rabbit; Cell Signaling), total P65 (6956, 1:1000 mouse; Cell Signaling), phospho-IκBα (2859, 1:1000 rabbit; Cell Signaling), and total IκBα (L35A5, 1:1000, mouse; Cell Signaling) were used. Secondary Abs were obtained from Cell Signaling Technology, and bands were detected using a chemiluminescence kit (Thermo Fisher Scientific, Waltham, MA). Densitometry analyses were carried out using the ImageJ software (National Institutes of Health, Bethesda, MD).

luminometry. (**C**) THP-$1^{NF\text{-}\kappa B}$ cells were pretreated with 250 μM DMOG for 1 h and stimulated with 1 μg/ml FSL-1 for 30 min. Phosphorylation of p65, IκBα, or β-actin levels were determined by Western blot. Densitometry values are shown as mean + SEM for $n = 3$ independent experiments. (**D**) Quantification of A20 expression in RNA extracted from THP-1 cells pretreated with 250 μM DMOG for 1 h and stimulated with 1 μg/ml of FSL-1 for 24 h. (**E**–**G**)THP-$1^{NF\text{-}\kappa B}$ reporter cells were pretreated with 10–1000 μM DMOG or the appropriate V prior to treatment with 10^9 cells/ml HKLM (C) 1 μg/ml LPS (D), 10 ng/ml of IL-1β (E), or V (F) for 24 h, and luciferase activity was measured by luminometry. Data are represented as mean + SEM. Statistical analysis was performed using a one-way ANOVA, followed by Tukey posttest. $n = 3$–4 independent experiments. $^*p \leq 0.05$, $^{**}p \leq 0.01$, $^{***}p \leq 0.001$, $^{****}p \leq 0.0001$.

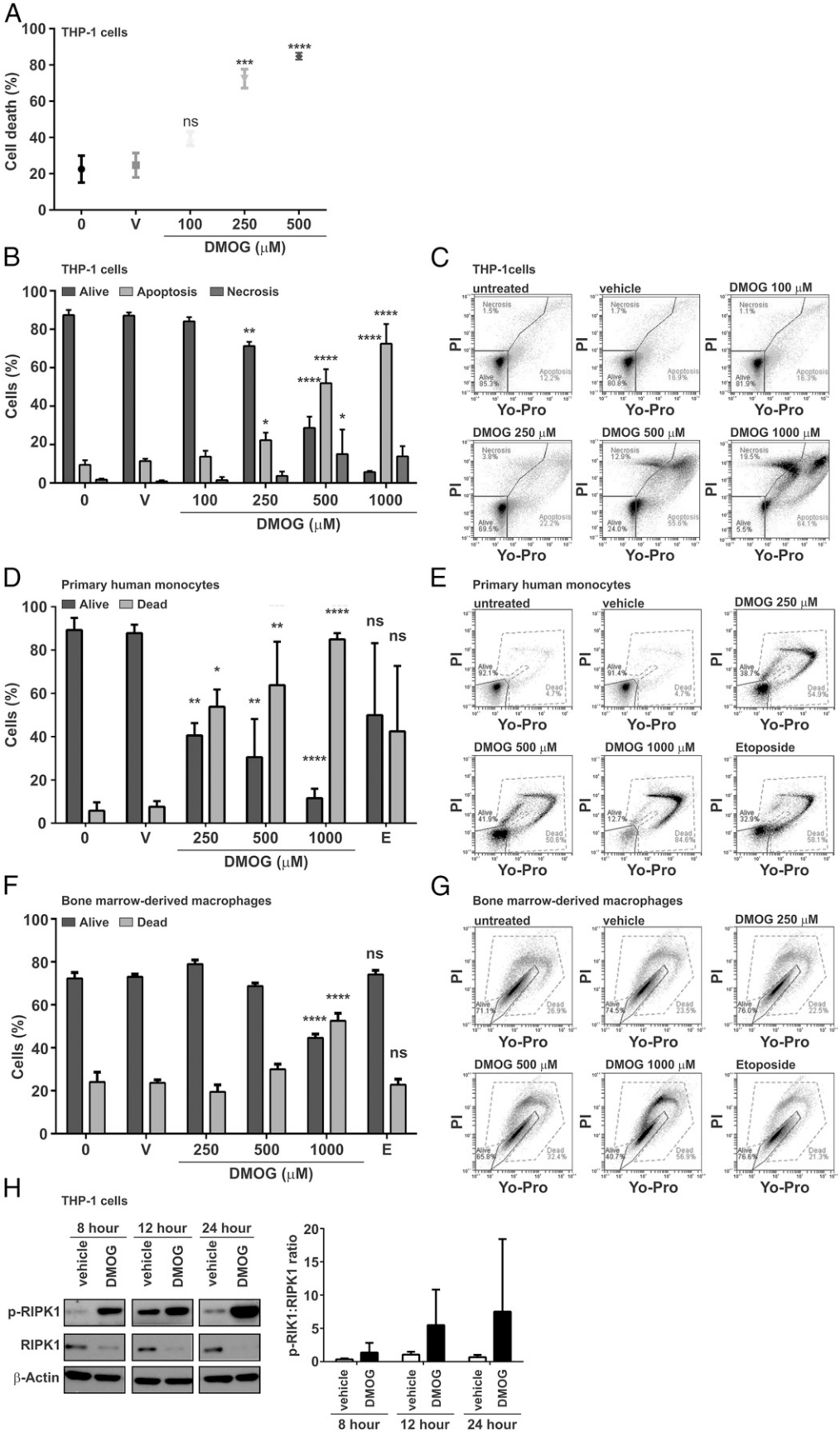

FIGURE 2. DMOG induces cell death in human monocytes. (**A**) LDH release assay to measure the impact of increasing concentrations of DMOG on THP-1 cell necrosis. (**B** and **C**) Flow cytometric analysis of DMOG- or etoposide-induced apoptosis in THP-1 cells. (**D** and **E**) Flow cytometric analysis of DMOG or etoposide apoptosis in primary human monocytes. (**F** and **G**) Flow cytometric analysis of DMOG or etoposide apoptosis in BMDMs. (**H**) Representative immunoblots reflecting RIPK1, phospho-RIPK1, and total RIPK1 proteins in THP-1 cells treated with vehicle or *(Figure legend continues)*

Real-time quantitative PCR

Total RNA was isolated with TRI Reagent (Sigma-Aldrich); cDNA was synthesized with Moloney Murine Leukemia Virus Reverse Transcriptase (Promega), according to the manufacturer's instructions. Target cDNAs were quantified using Applied Biosystems QuantStudio 7 Flex Real-Time PCR system, thermal cycle was 10 min at 95°C once, 15 s at 95°C, and 1 min at 60°C, repeated for 40 cycles. TaqMan probes (Thermo Fisher Scientific) used were as follows: BIRC2 (Hs01112284_m1), TNFAIP3 (Hs00234713_m1), and eukaryotic 18S rRNA (4310893E). The relative expression of each of the genes was analyzed using the δ-δ Ct method.

Caspase assay

The caspase-3/7 activity assay was performed as described previously (25). Briefly, 7.5×10^5 THP-1 cells or 1×10^6 HEK 293 or MEF cells were seeded, respectively, in 12-well plate or in 60-mm dishes. Monocytes were seeded in duplicate for each treatment in a final volume of 1250 μl fresh medium per well. HEK 293 and MEF cells were, instead, seeded in a final volume of 2500 μl/dish. After treatment, cells were gently scraped and collected in prechilled tubes and spun at 1100 rpm at 4°C for 5 min. The supernatant was removed, and cells were washed once in 1 ml of ice-cold PBS. Subsequently, cells were centrifuged at 1100 rpm at 4°C for 5 min. After removal of PBS, cells were lysed with 100 μl of ice-cold caspase assay lysis buffer containing glycerol 10%, CHAPS 0.5%, EDTA 0.5 mM (pH 8), PMSF 0.1 mM, and DTT 5 mM, prepared in a final volume of 50 ml PBS, and stored in −20°C until the assay was performed. Prior to analysis, samples were removed from −20°C and allowed to thaw at room temperature. Eighty microliters of lysate was pipetted into a black 96-well plate and incubated with 100 μM Ac-DEVD-AMC diluted in CALB. The protease activity was then measured at $\lambda_{ex}/\lambda_{em}$ = 400/505 nm using a SpectraMax190 Microplate Reader (Molecular Devices, Sunnyvale, CA). The assay was performed at 37°C, and the plate was assayed for 121 cycles with 1-min intervals.

Lactate dehydrogenase assay

The lactate dehydrogenase (LDH) assay was carried out according to the manufacturer's instructions (catalog no. 11644793001; Roche, Basel, Switzerland).

Flow cytometry analysis

HEK 293, MEF, Jurkat, THP-1, BMDM cells and primary human monocytes from healthy donors were incubated with YoPro (YP) and propidium iodide (PI) (Vybrant Apoptosis Assay Kit no.4 V13243; Invitrogen, Thermo Fisher Scientific) and subjected to flow cytometric analysis using the BD Accuri C6 flow cytometer (BD Bioscience) and CFlow software (version 1.0.264.21). For these experiments, we used wild-type THP-1 cells because of the incompatibility of the endogenous luciferase of THP-1$^{NF\text{-}\kappa B}$ cells and the fluorescent dyes used. A total of 7.5×10^6 HEK 293, MEF, Jurkat, and THP-1 cells were seeded and analyzed for each treatment; 2.0×10^4 primary human monocytes were seeded and analyzed for each treatment; and 3×10^6 BMDM cells were seeded and analyzed for each treatment. A minimum of two replicates per experiment were performed. Positive control stimuli of apoptosis and necrosis (etoposide and cadmium chloride, respectively), were used to establish a gating strategy (Supplemental Fig. 1A–C). Gates were established individually for each of the cells types according to the biological controls.

Statistical analysis

Data are shown as mean ± SEM for all indicated independent experiments. Statistical significance was evaluated by using one- or two-way ANOVA, followed by Tukey posttest. Asterisks denote the level of significance as follows: *$p \leq 0.05$, **$p \leq 0.01$, ***$p \leq 0.001$, and ****$p \leq 0.0001$; $p \geq 0.05$ is NS.

Results

Hydroxylase inhibition attenuates TLR-mediated NF-κB activity

We first investigated the impact of pharmacologic hydroxylase inhibition on HIF-1α stability in monocytes. THP-1$^{NF\text{-}\kappa B}$ cells were incubated with DMOG (100–250 μM) for 24 h. Western blot with accompanying densitometry analysis revealed a dose-dependent stabilization of HIF-1α, reflecting responsiveness of these cells to pharmacologic hydroxylase inhibition (Fig. 1A). We next investigated the effect of hydroxylase inhibition on TLR-induced NF-κB signaling. THP-1$^{NF\text{-}\kappa B}$ cells were pretreated with 250 μM DMOG for 1 h prior to stimulation with a range of TLR agonists: 10^9 cells/ml HKLM (TLR2 agonist), 1 μg/ml LPS (TLR4 agonist), 1 μg/ml Pam3CSK4 (TLR1/2 agonist), 1 μg/ml FLA-ST (TLR5 agonist), or 1 μg/ml FSL-1 (TLR2/6 agonist). For positive controls, cells were stimulated with 10 ng/ml of IL-1β (IL-1R) or 1 μg/ml of LIGHT (26). NF-κB activity was measured 24 h following agonist stimulation. All TLR agonists increased NF-κB transcriptional activity and, in all cases, this was attenuated in DMOG-treated cells (Fig. 1B). A similar inhibitory effect was observed using an alternative hydroxylase inhibitor EDHB (Supplemental Fig. 2A, 2B).

We next investigated the effects of DMOG treatment on the endogenous NF-κB pathway. First, we investigated the impact of DMOG treatment on the expression level of the NF-κB–dependent TNFA1P3 gene (which encodes A20) by real-time quantitative PCR. FSL-1 induced an increase of A20, as previously described (27, 30). However, treatment with DMOG did not affect TNFA1P3 expression, indicating that residual NF-κB activity was sufficient for full expression of this gene (data not shown). We next investigated the impact of DMOG on phosphorylation of p65 and IκBα by Western blot. Cells exposed to FSL-1 showed an increase in phosphorylation of both p65 and IκBα, reflecting NF-κB activation. DMOG treatment reduced FSL-1–induced phosphorylation of IκBα, thus supporting an inhibition of canonical NF-κB signaling by hydroxylase inhibition (Fig. 1C).

To investigate whether the effects of hydroxylase inhibition on TLR-induced NF-κB activity were dose dependent, we treated THP-1$^{NF\text{-}\kappa B}$ cells with 10 μM–1 mM DMOG for 1 h in advance of the stimulation with 10^9 cells/ml HKLM (TLR2 agonist), 1 μg/ml LPS (TLR4 agonist), or 10 ng/ml IL-1β for 24 h, and the NF-κB transcriptional activity was measured. We found that DMOG inhibited TLR2-, TLR4-, and IL-1R–mediated NF-κB transcriptional activity in a dose-dependent manner in monocytes (Fig. 1D–G). Furthermore, a dose-dependent decrease of the basal NF-κB activity in unstimulated THP-1$^{NF\text{-}\kappa B}$ cells was also observed (Fig. 1G). In summary, pharmacologic hydroxylase inhibition reduced basal and stimulated TLR-induced NF-κB signaling in human monocytes independently of the nature of stimuli used.

Hydroxylase inhibition reduces the viability of human monocytes

Given the broad and apparently stimulus-independent nature of the inhibitory effect of hydroxylase inhibition on NF-κB activity, we next investigated the possibility that DMOG treatment may impact monocyte viability. In these studies, necrosis was identified by LDH release assay and YP assay (high ratio of PI uptake), apoptosis was identified by increased caspase activity and YP assay (low ratio of PI uptake), and necroptosis was identified by the phosphorylation of RIPK.

1000 μM DMOG for time indicated. Densitometry data of phospho-RIPK/pan-RIPK are expressed as mean + SEM of $n = 4$ independent experiments. In all immunoblots, β-actin was used as positive control. Densitometry data of cIAP1 levels are expressed as mean + SEM of $n = 3$ independent experiments. Data are expressed as mean percentage of live, apoptotic, and necrotic populations + SEM ($n = 4$). Statistical analysis was performed using one- or two-way ANOVA, followed by Tukey posttest. *$p \leq 0.05$, **$p \leq 0.0$, ***$p \leq 0.001$, ****$p \leq 0.0001$.

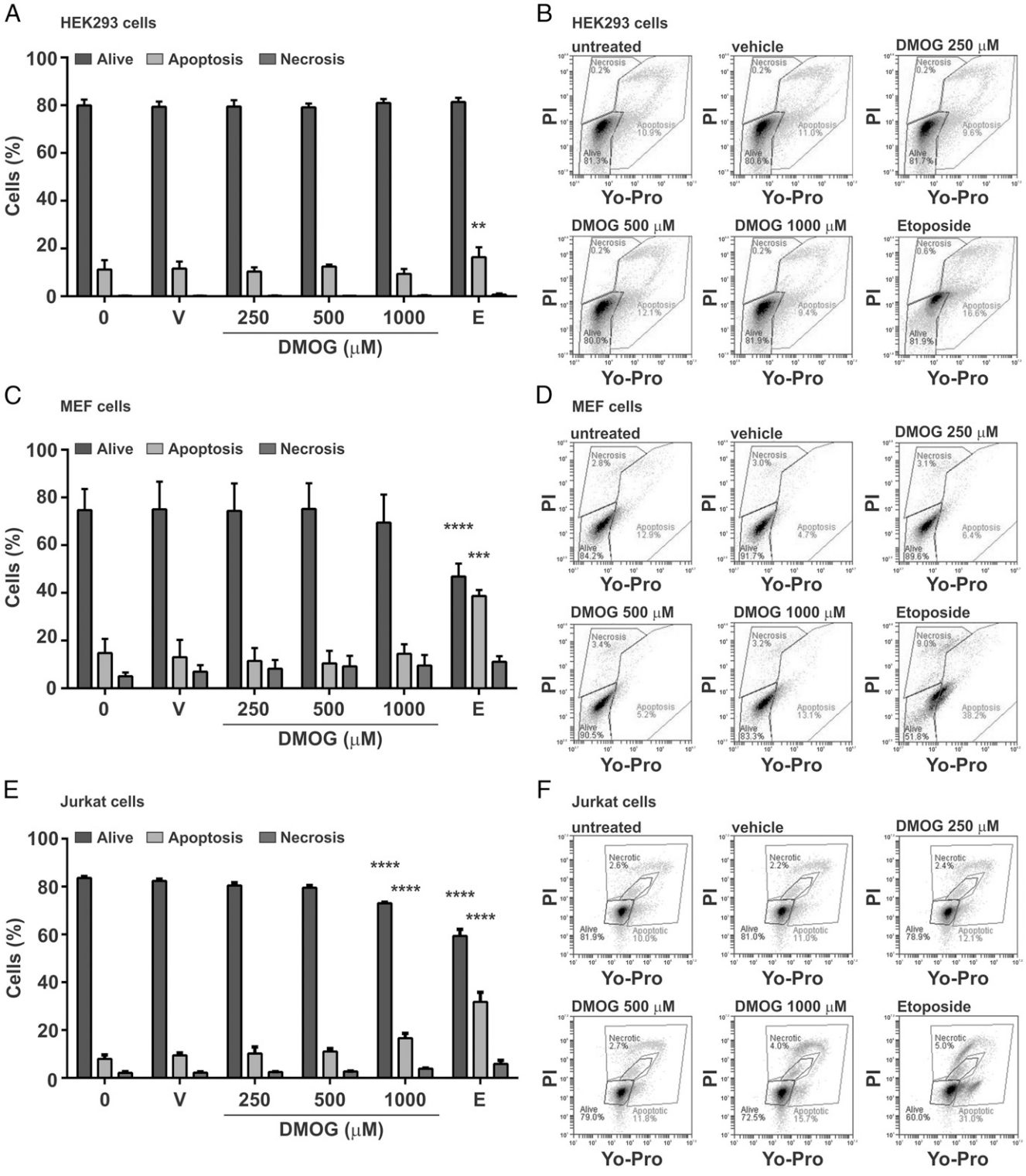

FIGURE 3. DMOG-induced apoptosis is selective for human monocytes. HEK 293 (**A** and **B**), MEF (**C** and **D**), and Jurkat cells (**E** and **F**) kept untreated (0) or cultured in the presence of DMSO vehicle (V) or DMOG for 24 h, as indicated in the figure. (A), (C), and (E) show quantification of flow cytometry analysis of HEK 293, MEF, and Jurkat cells, respectively. (B), (D), and (F) show representative density plots of flow cytometry analyses quantified in (A), (C), and (E), respectively. Fifteen-micromolar etoposide (E) was used as positive control. Data are expressed as mean percentage of live, apoptotic, and necrotic population + SEM ($n = 4$). Statistical analysis was performed using two-way ANOVA, followed by Tukey posttest. The asterisk (*) denotes the significance over the control, $n = 3$–5. $^{**}p \leq 0.01$, $^{***}p \leq 0.001$, $^{****}p \leq 0.0001$.

Cells were treated with 100–500 μM DMOG for 24 h. DMOG treatment led to a dose-dependent increase in cell death in THP-1 cells, as reflected by LDH release (Fig. 2A).

We next investigated the impact of hydroxylase inhibition on monocyte apoptosis. For these studies, cells were treated with DMOG for 24 h, and viability was assessed by flow cytometry using the YP/PI exclusion method for the detection of apoptotic cells (Supplemental Fig. 1). We found that THP-1 apoptosis was induced in a dose-dependent manner in response to DMOG treatment (Fig. 2B). Cells treated with low concentrations of

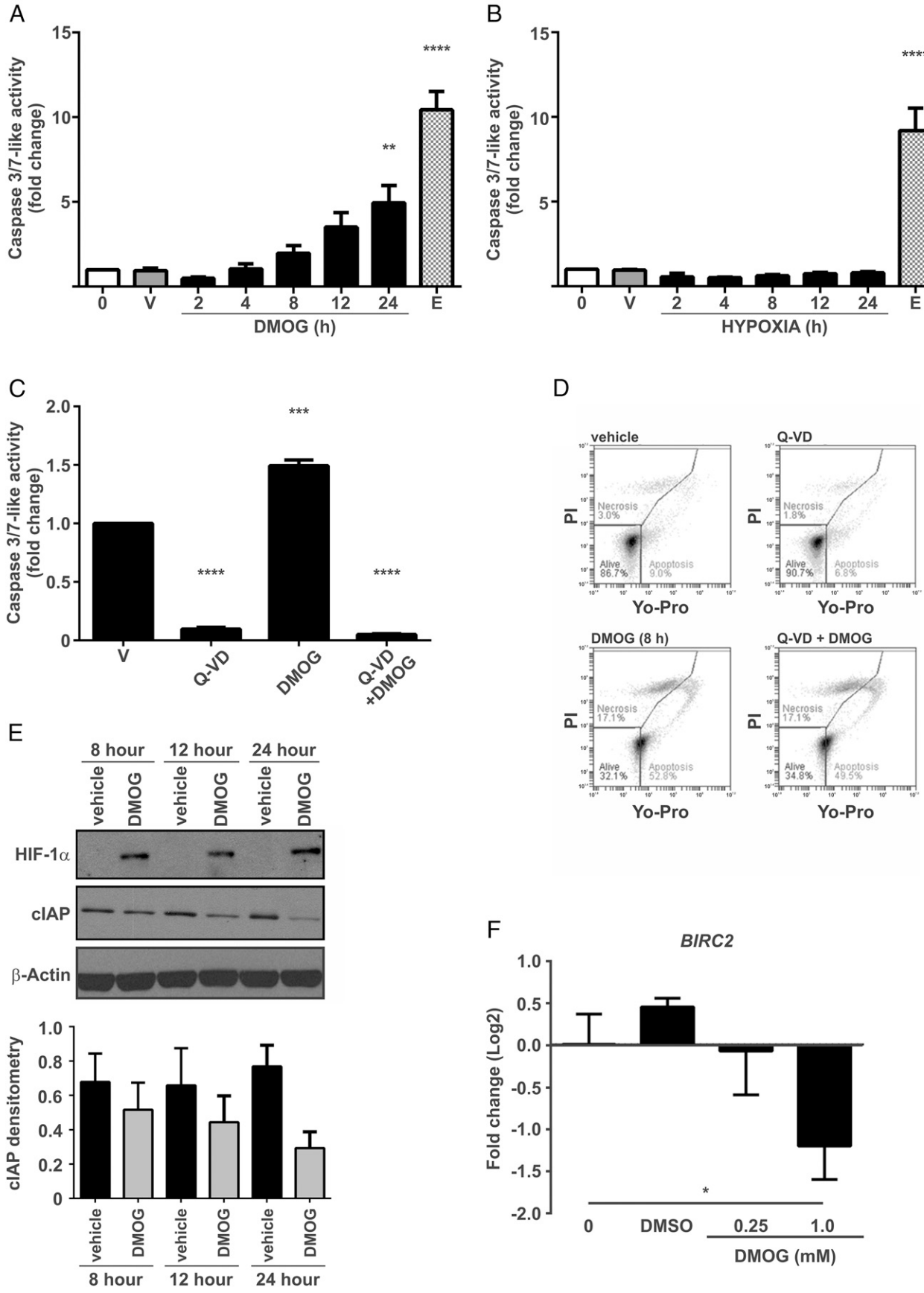

FIGURE 4. DMOG induces monocytes death through a caspase-independent mechanism. THP-1 cells were kept untreated (0) or cultured in the presence of vehicle (V), 15 μM etoposide (E), or 1 mM DMOG (**A**) or exposed to hypoxia (**B**) for times indicated, and caspase activity was measured. (**C**) THP-1 cells were pretreated with 10 μM the pan-caspase inhibitor Q-VD for 1 h and incubated for further 8 h with 1 mM DMOG, and the caspase activity was measured (**D**). Flow cytometry analyses of THP-1 treated as in (C) using YP/PI strategy. Data in (A)–(C) shown as + SEM. (**E**) *(Figure legend continues)*

DMOG (100–250 μM) predominantly underwent early apoptosis, whereas cells treated with higher concentrations (500–1000 μM) displayed markers of late stage apoptosis/necrosis characterized by damaged membrane integrity (Fig. 2C). These data indicate that DMOG provokes cell death through apoptosis in THP-1 cells.

We next investigated whether the proapoptotic effect of DMOG was recapitulated in primary human monocytes isolated from healthy donors. Primary human monocytes were treated with 250–1000 μM DMOG for 24 h. We found that, similar to THP-1 cells, DMOG induced apoptosis in primary human monocytes (Fig. 2D, 2E). Next, we investigated the effect of DMOG treatment on differentiated macrophages. Murine BMDM on day 7 of differentiation were incubated with DMOG (250–1000 μM) for 24 h. Interestingly, differentiated macrophages demonstrated resistance to DMOG-induced cell death, compared with undifferentiated monocytes (Fig. 2F, 2G). To determine whether the effects observed were specific for hydroxylase inhibition with DMOG, THP-1 cells were also exposed to increasing concentrations of the alternative hydroxylase inhibitor EDHB (250–1000 μM). LDH assay showed that EDHB did not increase the rate of necrosis significantly in human monocytes (Supplemental Fig. 3A). To further evaluate the impact of EDHB on THP-1, samples were subjected to flow cytometry as well. Cells treated with 1 mM EDHB showed significantly increased cell death, although not as pronounced as that of DMOG (Supplemental Fig. 3B, 3C). Data also showed that these cells were at early stage of apoptosis, supporting the data obtained from the LDH assay (Supplemental Fig. 3A), which demonstrated only small increases in necrotic cells, indicating that EDHB causes cell death only through apoptosis (Supplemental Fig. 3B, 3C). An effect similar to DMOG and EDHB on monocyte survival was also found in response to treatment with JNJ1935, an alternative hydroxylase inhibitor (Supplemental Fig. 3D–F).

We next investigated the impact of hydroxylase inhibition on monocyte necroptosis, a distinct and recently described mode of cell death with characteristics of both necrosis and apoptosis. Phosphorylation of RIPK1 is a hallmark of necroptosis (31, 32). We tested whether DMOG regulates phosphorylation of RIPK1 in human monocytes. Immunoblot analysis was performed in THP-1 cells treated with 1 mM DMOG for 8, 12, and 24 h. We found that DMOG treatment resulted in an increase in RIPK1 phosphorylation (Fig. 2H). Taken together, these data demonstrate that monocytes are highly sensitive to the induction of cell death through necrosis, apoptosis, and necroptosis in response to pharmacologic hydroxylase inhibition.

DMOG selectively induces cell death in human monocytes

To investigate whether the DMOG-induced cell death was selective for monocytes, we next assessed the impact of hydroxylase inhibition on cell death in other cell types, including human kidney epithelial cells, MEF cells, and T lymphocytes (Jurkat). HEK 293, MEF, and Jurkat cells were treated with DMOG (250–1000 μM) for 24 h. DMOG treatment did not induce cell death in either HEK 293 (Fig. 3A, 3B) or MEF (Fig. 3C, 3D) cells at any concentration tested. Jurkat cells showed a moderate, but significant, increase in cell death only with 1 mM DMOG (Fig. 3E, 3F). These data suggest that the DMOG-mediated induction of cell death is selective for monocytes.

DMOG induces monocyte death through a caspase-independent mechanism

We next investigated mechanistic aspects of the induction of monocyte apoptosis in response to hydroxylase inhibition. Induction of apoptosis is generally mediated through activation of the caspase cascade (33). To test if DMOG activates the executioner caspase-3 and -7, THP-1 cells were treated with 1000 μM DMOG (Fig. 4A) or exposed to hypoxia (1% O_2/5% CO_2/balance N_2; Fig. 4B) for 0–24 h. Control cells were also treated with 15 μM etoposide, a known inducer of caspase-dependent apoptosis. DMOG increased caspase-3/7–like activity in THP-1 cells in a time-dependent manner (Fig. 4A). Etoposide treatment increased caspase-3/7–like activity by 10.9-fold, which is 5.9-fold higher than that of in DMOG-treated cells. Hypoxia did not increase caspase-3/7 activity after 24 h (Fig. 4B). We next investigated whether the DMOG-induced monocyte death is dependent on caspase activation using the caspase inhibitor Q-VD. The ability of Q-VD to inhibit caspase-3/7–like activity and rescue monocytes from apoptosis was confirmed in cells treated with etoposide (Supplemental Fig. 4A, 4B). THP-1 cells were pretreated with 10 μM Q-VD for 1 h and subsequently exposed to 1 mM DMOG for 8 h. Cells were then analyzed by caspase-3/7 assay or flow cytometry. Q-VD fully inhibited caspase-3/7–like activity in DMOG-treated cells (Fig. 4C). However, Q-VD treatment did not prevent DMOG-induced apoptosis (Fig. 4D). These data suggest the existence of a caspase-independent apoptotic mechanism in hydroxylase inhibitor–treated human monocytes. Of interest, DMOG treatment markedly downregulated the expression of the antiapoptotic protein cIAP1, indicating that this may, at least in part, drive the proapoptotic effects of hydroxylase inhibition in monocytes (Fig. 4E). To assess whether the reduction of cIAP1 protein levels was consequence of reduced gene expression, we performed a real-time quantitative PCR of cIAP1 gene (known as BIRC2). THP-1 cells treated with 250 and 1000 μM DMOG for 6 h showed reduced level of mRNA, indicating that DMOG affects the gene expression of BIRC2 (Fig. 4F). In conclusion, DMOG selectively induces multiple forms of cell death in human monocytes in a manner that is accompanied by depletion of cIAP1 and phosphorylation of RIPK1.

Discussion

HIF-hydroxylases (PHD/FIH) are key regulators of the stability and activity of the HIF (5). However, mounting evidence now indicates that these enzymes also regulate components of other pathways, including NF-κB (34, 35). Hydroxylase inhibition ameliorates inflammation in preclinical models of inflammatory bowel disease. Because TLRs expressed on mucosal immune cells are heavily activated during inflammatory bowel disease, the aim of the current study was to gain insight into the impact of hydroxylase inhibitors on TLR-induced NF-κB signaling. We observed a widespread and stimulus-independent attenuation of TLR-induced NF-κB signaling in human monocytes upon treatment with the hydroxylase inhibitors DMOG and EDHB. Activity of NF-κB is controlled by the IκB kinase (IKK) complex (36). In response to infection or inflammatory stimuli, the IKK complex is phosphorylated and activated and, in turn, mediates the phosphorylation-dependent degradation of the IκBα. This liberates NF-κB, which, in turn, regulates inflammatory gene

Representative immunoblots reflecting HIF-1α and cIAP1 proteins of THP-1 cells treated with vehicle or 1 mM DMOG for times indicated. Densitometry data of cIAP1 levels are also shown for $n = 4$ independent experiments. (**F**) Quantification of cIPA1 expression in RNA extracted from THP-1 cells treated with 250 μM–1 mM DMOG for 6 h. Statistical analysis was performed with one-way ANOVA, followed by Tukey posttest. $n = 3$ independent experiments. $^{*}p \leq 0.1$, $^{**}p \leq 0.01$, $^{***}p \leq 0.001$, $^{****}p \leq 0.0001$.

expression (37–39). Previous work has shown a functional role of hydroxylases in regulating IKK activity (34). Consistent with this study, our Western blot analyses show that DMOG attenuates NF-κB signaling, at least in part, by reducing IκBα phosphorylation.

Because of the broad inhibitory effect of DMOG on NF-κB activity in monocytes, we next investigated whether DMOG may affect monocyte viability. Viability assays demonstrated that human monocyte cultures are highly sensitive to hydroxylase inhibition. This finding was unexpected as it has been previously demonstrated that pharmacological inhibition of HIF-hydroxylases by DMOG promotes cell survival in other cell types including neurons (40, 41), neutrophils (42), hepatocytes (43), alveolar epithelial cells (44, 45), and bone marrow–derived mesenchymal stem cells (46). Consistent with these studies, we found that DMOG did not impact viability of other cell types, including HEK 293, MEF, and Jurkat cells.

Although monocytes are precursors of macrophages, the expression of NF-κB family members is higher in macrophages than in undifferentiated cells (47, 48). Furthermore, macrophages typically have a longer life span than monocytes. As monocytes differentiate into macrophages, there is an upregulation of endogenous inhibitors of cell death (e.g., XIAP and cFLIP), and this promotes resistance to cell death pathways (49). Considering that NF-κB drives the synthesis of antiapoptotic genes such as cIAP1 (50) or cFLIP (51), this might provide an explanation for the relative resistance of the differentiated BMDMs to DMOG treatment when compared with undifferentiated THP-1 cells or primary human monocytes.

It remains to be determined whether the anti-inflammatory effect of hydroxylase inhibitors might be, in part, a consequence of reduced levels of circulating monocytes in models of intestinal inflammation. It has recently been demonstrated that DMOG treatment reduces neutrophil numbers in a model of allergic contact dermatitis through increased levels of apoptosis (52).

Caspases-3 and -7 play pivotal roles in the induction of caspase-dependent apoptosis (53). We found the increase of the caspase-3/7–like activity in a time-dependent manner in response to hydroxylase inhibition, but not to hypoxia. However, the caspase inhibitor failed to prevent DMOG-induced cell death, indicating a caspase-independent mechanism of DMOG-induced apoptosis in monocytes, which shares some characteristics with necroptosis.

IAP proteins are primarily involved in inhibition of caspase activity (54). In addition, cIAP1 is a regulator of NF-κB signaling and macrophage necroptosis (31). Under survival conditions, RIPK1 is ubiquitylated by cIAP1 and -2 (55, 56), resulting in NF-κB activation. Recently, it was shown that, in the absence of cIAP1, RIPK1 becomes deubiquitylated and forms an active kinase involved in the downstream events of caspase-independent necroptosis (57).

In monocytes, we found that DMOG treatment decreases cIAP1 levels and increases RIPK1 phosphorylation, both markers of necroptosis. As previously described, NF-κB drives the transcription of genes involved in cell survival, one of which is cIAP1 (50, 57). Thus, downregulation of cIAP1 might be, at least in part, mediated by reduced NF-κB transcriptional activity in THP-1 cells exposed to DMOG. cIAP1 levels, in turn, would not be sufficient to counteract the activity of caspase-3/7, and this might explain the activation of caspase-3/7 in DMOG-treated monocytes. However, in monocytes exposed to hypoxia, we found no increase of the caspase-3/7–like activity. Previous reports by other groups suggested that hypoxia activates NF-κB in endothelial cells (58). Consistent with this work, in our system, hypoxia enhanced basal and TLR agonist–induced NF-κB transcriptional activity in hypoxic cells compared with normoxic cells (data not shown). Therefore, we cannot exclude the possibility that in hypoxia, HIF, and NF-κB might synergistically mediate adaptation of monocytes to anaerobic metabolism, as previously suggested in other models. In support of this idea, under hydroxylase inhibition with DMOG or hypoxia, neutrophils have been reported to have increased survival at the site of infection via HIF-1–dependent upregulation of NF-κB activity (42).

In conclusion, we demonstrated that, in monocytes, the α-KG mimetic DMOG reduces basal and TLR-induced NF-κB transcriptional activity and regulates cell death through a caspase-independent mechanism in human monocytes. These data implicate a role for HIF-hydroxylases in mediating the effects of pharmacologic hydroxylase inhibition on monocyte cell death. However, we cannot rule out roles for other 2-oxogluterate–dependent dioxygenases given the lack of isoform specificity of the agents used. DMOG induces a reduction in cIAP1 levels and phosphorylation of RIPK1 markers of necroptosis. Further analysis on the effects of DMOG on monocytes survival in vivo might shed light on the selective sensitivity of monocytes. These data contribute to our understanding of the anti-inflammatory effects of hydroxylase inhibitors in chronic inflammatory disease.

Acknowledgments

We acknowledge the assistance of Dr. Mohamed Ismaiel.

Disclosures

C.T.T. is a Scientific Advisory Board Member of Akebia Therapeutics. The other authors have no financial conflicts of interest.

References

1. Taylor, C. T. 2008. Mitochondria and cellular oxygen sensing in the HIF pathway. *Biochem. J.* 409: 19–26.
2. Wang, G. L., and G. L. Semenza. 1995. Purification and characterization of hypoxia-inducible factor 1. *J. Biol. Chem.* 270: 1230–1237.
3. Kaelin, W. G., Jr., and P. J. Ratcliffe. 2008. Oxygen sensing by metazoans: the central role of the HIF hydroxylase pathway. *Mol. Cell* 30: 393–402.
4. Bruick, R. K., and S. L. McKnight. 2001. A conserved family of prolyl-4-hydroxylases that modify HIF. *Science* 294: 1337–1340.
5. Schofield, C. J., and P. J. Ratcliffe. 2004. Oxygen sensing by HIF hydroxylases. *Nat. Rev. Mol. Cell Biol.* 5: 343–354.
6. Jaakkola, P., D. R. Mole, Y. M. Tian, M. I. Wilson, J. Gielbert, S. J. Gaskell, A. von Kriegsheim, H. F. Hebestreit, M. Mukherji, C. J. Schofield, et al. 2001. Targeting of HIF-alpha to the von Hippel-Lindau ubiquitylation complex by O2-regulated prolyl hydroxylation. *Science* 292: 468–472.
7. Lando, D., D. J. Peet, J. J. Gorman, D. A. Whelan, M. L. Whitelaw, and R. K. Bruick. 2002. FIH-1 is an asparaginyl hydroxylase enzyme that regulates the transcriptional activity of hypoxia-inducible factor. *Genes Dev.* 16: 1466–1471.
8. Hagen, T., C. T. Taylor, F. Lam, and S. Moncada. 2003. Redistribution of intracellular oxygen in hypoxia by nitric oxide: effect on HIF1alpha. *Science* 302: 1975–1978.
9. Taylor, C. T. 2008. Interdependent roles for hypoxia inducible factor and nuclear factor-kappaB in hypoxic inflammation. *J. Physiol.* 586: 4055–4059.
10. Akira, S., S. Uematsu, and O. Takeuchi. 2006. Pathogen recognition and innate immunity. *Cell* 124: 783–801.
11. Crifo, B., and C. T. Taylor. 2016. Crosstalk between toll-like receptors and hypoxia-dependent pathways in health and disease. *J. Investig. Med.* 64: 369–375.
12. Dixit, V. M., S. Green, V. Sarma, L. B. Holzman, F. W. Wolf, K. O'Rourke, P. A. Ward, E. V. Prochownik, and R. M. Marks. 1990. Tumor necrosis factor-alpha induction of novel gene products in human endothelial cells including a macrophage-specific chemotaxin. *J. Biol. Chem.* 265: 2973–2978.
13. Ruland, J. 2011. Return to homeostasis: downregulation of NF-κB responses. *Nat. Immunol.* 12: 709–714.
14. Scholz, C. C., M. A. Cavadas, M. M. Tambuwala, E. Hams, J. Rodríguez, A. von Kriegsheim, P. Cotter, U. Bruning, P. G. Fallon, A. Cheong, et al. 2013. Regulation of IL-1β-induced NF-κB by hydroxylases links key hypoxic and inflammatory signaling pathways. *Proc. Natl. Acad. Sci. USA* 110: 18490–18495.
15. Hams, E., S. P. Saunders, E. P. Cummins, A. O'Connor, M. T. Tambuwala, W. M. Gallagher, A. Byrne, A. Campos-Torres, P. M. Moynagh, C. Jobin, et al. 2011. The hydroxylase inhibitor dimethyloxallyl glycine attenuates endotoxic shock via alternative activation of macrophages and IL-10 production by B1 cells. *Shock* 36: 295–302.

16. Eltzschig, H. K., D. L. Bratton, and S. P. Colgan. 2014. Targeting hypoxia signalling for the treatment of ischaemic and inflammatory diseases. *Nat. Rev. Drug Discov.* 13: 852–869.
17. Fraisl, P., J. Aragonés, and P. Carmeliet. 2009. Inhibition of oxygen sensors as a therapeutic strategy for ischaemic and inflammatory disease. *Nat. Rev. Drug Discov.* 8: 139–152.
18. Mole, D. R., I. Schlemminger, L. A. McNeill, K. S. Hewitson, C. W. Pugh, P. J. Ratcliffe, and C. J. Schofield. 2003. 2-oxoglutarate analogue inhibitors of HIF prolyl hydroxylase. *Bioorg. Med. Chem. Lett.* 13: 2677–2680.
19. Wang, J., J. L. Buss, G. Chen, P. Ponka, and K. Pantopoulos. 2002. The prolyl 4-hydroxylase inhibitor ethyl-3,4-dihydroxybenzoate generates effective iron deficiency in cultured cells. *FEBS Lett.* 529: 309–312.
20. Cummins, E. P., F. Seeballuck, S. J. Keely, N. E. Mangan, J. J. Callanan, P. G. Fallon, and C. T. Taylor. 2008. The hydroxylase inhibitor dimethyloxalylglycine is protective in a murine model of colitis. *Gastroenterology* 134: 156–165.
21. Akira, S., K. Takeda, and T. Kaisho. 2001. Toll-like receptors: critical proteins linking innate and acquired immunity. *Nat. Immunol.* 2: 675–680.
22. Pandey, S., T. Kawai, and S. Akira. 2014. Microbial sensing by Toll-like receptors and intracellular nucleic acid sensors. *Cold Spring Harb. Perspect. Biol.* 7: a016246.
23. Kobe, B., and J. Deisenhofer. 1995. Proteins with leucine-rich repeats. *Curr. Opin. Struct. Biol.* 5: 409–416.
24. Blasius, A. L., and B. Beutler. 2010. Intracellular toll-like receptors. *Immunity* 32: 305–315.
25. Fabian, Z., P. O'Brien, K. Pajecka, and H. O. Fearnhead. 2009. TPCK-induced apoptosis and labelling of the largest subunit of RNA polymerase II in Jurkat cells. *Apoptosis* 14: 1154–1164.
26. Aggarwal, B. B., S. C. Gupta, and J. H. Kim. 2012. Historical perspectives on tumor necrosis factor and its superfamily: 25 years later, a golden journey. *Blood* 119: 651–665.
27. Catrysse, L., L. Vereecke, R. Beyaert, and G. van Loo. 2014. A20 in inflammation and autoimmunity. *Trends Immunol.* 35: 22–31.
28. Negishi, H., Y. Fujita, H. Yanai, S. Sakaguchi, X. Ouyang, M. Shinohara, H. Takayanagi, Y. Ohba, T. Taniguchi, and K. Honda. 2006. Evidence for licensing of IFN-gamma-induced IFN regulatory factor 1 transcription factor by MyD88 in Toll-like receptor-dependent gene induction program. *Proc. Natl. Acad. Sci. USA* 103: 15136–15141.
29. Finucane, O. M., C. L. Lyons, A. M. Murphy, C. M. Reynolds, R. Klinger, N. P. Healy, A. A. Cooke, R. C. Coll, L. McAllan, K. N. Nilaweera, et al. 2015. Monounsaturated fatty acid-enriched high-fat diets impede adipose NLRP3 inflammasome-mediated IL-1β secretion and insulin resistance despite obesity. *Diabetes* 64: 2116–2128.
30. Verstrepen, L., K. Verhelst, G. van Loo, I. Carpentier, S. C. Ley, and R. Beyaert. 2010. Expression, biological activities and mechanisms of action of A20 (TNFAIP3). *Biochem. Pharmacol.* 80: 2009–2020.
31. McComb, S., H. H. Cheung, R. G. Korneluk, S. Wang, L. Krishnan, and S. Sad. 2012. cIAP1 and cIAP2 limit macrophage necroptosis by inhibiting Rip1 and Rip3 activation. *Cell Death Differ.* 19: 1791–1801.
32. Müller-Sienerth, N., L. Dietz, P. Holtz, M. Kapp, G. U. Grigoleit, C. Schmuck, H. Wajant, and D. Siegmund. 2011. SMAC mimetic BV6 induces cell death in monocytes and maturation of monocyte-derived dendritic cells. *PLoS One* 6: e21556.
33. Elmore, S. 2007. Apoptosis: a review of programmed cell death. *Toxicol. Pathol.* 35: 495–516.
34. Cummins, E. P., E. Berra, K. M. Comerford, A. Ginouves, K. T. Fitzgerald, F. Seeballuck, C. Godson, J. E. Nielsen, P. Moynagh, J. Pouyssegur, and C. T. Taylor. 2006. Prolyl hydroxylase-1 negatively regulates IkappaB kinase-beta, giving insight into hypoxia-induced NFkappaB activity. *Proc. Natl. Acad. Sci. USA* 103: 18154–18159.
35. Oliver, K. M., J. F. Garvey, C. T. Ng, D. J. Veale, U. Fearon, E. P. Cummins, and C. T. Taylor. 2009. Hypoxia activates NF-kappaB-dependent gene expression through the canonical signaling pathway. *Antioxid. Redox Signal.* 11: 2057–2064.
36. Tambuwala, M. M., E. P. Cummins, C. R. Lenihan, J. Kiss, M. Stauch, C. C. Scholz, P. Fraisl, F. Lasitschka, M. Mollenhauer, S. P. Saunders, et al. 2010. Loss of prolyl hydroxylase-1 protects against colitis through reduced epithelial cell apoptosis and increased barrier function. *Gastroenterology* 139: 2093–2101.
37. Hayden, M. S., and S. Ghosh. 2008. Shared principles in NF-kappaB signaling. *Cell* 132: 344–362.
38. Häcker, H., and M. Karin. 2006. Regulation and function of IKK and IKK-related kinases. *Sci. STKE* 2006: re13.
39. Luo, J. L., H. Kamata, and M. Karin. 2005. IKK/NF-kappaB signaling: balancing life and death--a new approach to cancer therapy. *J. Clin. Invest.* 115: 2625–2632.
40. Lee, S., E. Nakamura, H. Yang, W. Wei, M. S. Linggi, M. P. Sajan, R. V. Farese, R. S. Freeman, B. D. Carter, W. G. Kaelin, Jr., and S. Schlisio. 2005. Neuronal apoptosis linked to EglN3 prolyl hydroxylase and familial pheochromocytoma genes: developmental culling and cancer. *Cancer Cell* 8: 155–167.
41. Lomb, D. J., J. A. Straub, and R. S. Freeman. 2007. Prolyl hydroxylase inhibitors delay neuronal cell death caused by trophic factor deprivation. *J. Neurochem.* 103: 1897–1906.
42. Walmsley, S. R., C. Print, N. Farahi, C. Peyssonnaux, R. S. Johnson, T. Cramer, A. Sobolewski, A. M. Condliffe, A. S. Cowburn, N. Johnson, and E. R. Chilvers. 2005. Hypoxia-induced neutrophil survival is mediated by HIF-1alpha-dependent NF-kappaB activity. *J. Exp. Med.* 201: 105–115.
43. Fitzpatrick, S. F., Z. Fábián, B. Schaible, C. R. Lenihan, T. Schwarzl, J. Rodriguez, X. Zheng, Z. Li, M. M. Tambuwala, D. G. Higgins, et al. 2016. Prolyl hydroxylase-1 regulates hepatocyte apoptosis in an NF-κB-dependent manner. *Biochem. Biophys. Res. Commun.* 474: 579–586.
44. Schaible, B., S. McClean, A. Selfridge, A. Broquet, K. Asehnoune, C. T. Taylor, and K. Schaffer. 2013. Hypoxia modulates infection of epithelial cells by *Pseudomonas aeruginosa*. *PLoS One* 8: e56491.
45. Nagamine, Y., K. Tojo, T. Yazawa, S. Takaki, Y. Baba, T. Goto, and K. Kurahashi. 2016. Inhibition of Prolyl hydroxylase attenuates Fas ligand-induced apoptosis and lung injury in mice. *Am. J. Respir. Cell Mol. Biol.* 55: 878–888.
46. Liu, X. B., J. A. Wang, X. Y. Ji, S. P. Yu, and L. Wei. 2014. Preconditioning of bone marrow mesenchymal stem cells by prolyl hydroxylase inhibition enhances cell survival and angiogenesis in vitro and after transplantation into the ischemic heart of rats. *Stem Cell Res. Ther.* 5: 111.
47. Italiani, P., and D. Boraschi. 2014. From monocytes to M1/M2 macrophages: phenotypical vs. functional differentiation. *Front. Immunol.* 5: 514.
48. Takashiba, S., T. E. Van Dyke, S. Amar, Y. Murayama, A. W. Soskolne, and L. Shapira. 1999. Differentiation of monocytes to macrophages primes cells for lipopolysaccharide stimulation via accumulation of cytoplasmic nuclear factor kappaB. *Infect. Immun.* 67: 5573–5578.
49. Rijal, D., A. Ariana, A. Wight, K. Kim, N. A. Alturki, Z. Aamir, E. S. Ametepe, R. G. Korneluk, C. Tiedje, M. B. Menon, et al. 2018. Differentiated macrophages acquire a pro-inflammatory and cell death-resistant phenotype due to increasing XIAP and p38-mediated inhibition of RipK1. *J. Biol. Chem.* 293: 11913–11927.
50. Hofer-Warbinek, R., J. A. Schmid, C. Stehlik, B. R. Binder, J. Lipp, and R. de Martin. 2000. Activation of NF-kappa B by XIAP, the X chromosome-linked inhibitor of apoptosis, in endothelial cells involves TAK1. *J. Biol. Chem.* 275: 22064–22068.
51. Micheau, O., S. Lens, O. Gaide, K. Alevizopoulos, and J. Tschopp. 2001. NF-kappaB signals induce the expression of c-FLIP. *Mol. Cell. Biol.* 21: 5299–5305.
52. Manresa, M. C., L. Smith, L. Casals-Diaz, R. R. Fagundes, E. Brown, P. Radhakrishnan, S. J. Murphy, B. Crifo, M. J. Strowitzki, D. N. Halligan, et al. 2018. Pharmacologic inhibition of hypoxia-inducible factor (HIF)-hydroxylases ameliorates allergic contact dermatitis. *Allergy.* DOI: 10.1111/all.13655.
53. Kumar, S., and M. F. Lavin. 1996. The ICE family of cysteine proteases as effectors of cell death. *Cell Death Differ.* 3: 255–267.
54. Birnbaum, M. J., R. J. Clem, and L. K. Miller. 1994. An apoptosis-inhibiting gene from a nuclear polyhedrosis virus encoding a polypeptide with Cys/His sequence motifs. *J. Virol.* 68: 2521–2528.
55. Mahoney, D. J., H. H. Cheung, R. L. Mrad, S. Plenchette, C. Simard, E. Enwere, V. Arora, T. W. Mak, E. C. Lacasse, J. Waring, and R. G. Korneluk. 2008. Both cIAP1 and cIAP2 regulate TNFalpha-mediated NF-kappaB activation. *Proc. Natl. Acad. Sci. USA* 105: 11778–11783.
56. Roy, N., Q. L. Deveraux, R. Takahashi, G. S. Salvesen, and J. C. Reed. 1997. The c-IAP-1 and c-IAP-2 proteins are direct inhibitors of specific caspases. *EMBO J.* 16: 6914–6925.
57. Gyrd-Hansen, M., and P. Meier. 2010. IAPs: from caspase inhibitors to modulators of NF-kappaB, inflammation and cancer. *Nat. Rev. Cancer* 10: 561–574.
58. Koong, A. C., E. Y. Chen, and A. J. Giaccia. 1994. Hypoxia causes the activation of nuclear factor kappa B through the phosphorylation of I kappa B alpha on tyrosine residues. *Cancer Res.* 54: 1425–1430.